Ruthenocuprates $RuSr_2(Eu,Ce)_2Cu_2O_{10-y}$: Intrinsic magnetic multilayers

I. Živković,[1] Y. Hirai,[2] B. H. Frazer,[2] M. Prester,[1,*] D. Drobac,[1] D. Ariosa,[3] H. Berger,[3] D. Pavuna,[3] G. Margaritondo,[3] I. Felner,[4] and M. Onellion[2,†]

[1]*Institute of Physics, Post Office Box 304, HR-10 000, Zagreb, Croatia*

[2]*Physics Department, University of Wisconsin, Madison, Wisconsin 53706*

[3]*Institut de Physique Appliquée, École Polytechnique Fédérale de Lausanne, CH-1012 Lausanne, Switzerland*

[4]*Racah Institute of Physics, Hebrew University, Jerusalem, Israel*

(Received 10 October 2001; revised manuscript received 29 November 2001; published 28 March 2002)

We report ac susceptibility data on $RuSr_2(Eu,Ce)_2Cu_2O_{10-y}$ (Ru-1222, Ce content $x=0.5$ and 1.0), $RuSr_2GdCu_2O_8$ (Ru-1212), and $SrRuO_3$. Both Ru-1222 ($x=0.5$, 1.0) sample types exhibit unexpected magnetic dynamics in low magnetic fields: logarithmic time relaxation, switching behavior, and ''inverted'' hysteresis loops. Neither Ru-1212 nor $SrRuO_3$ exhibit such magnetic dynamics. The results are interpreted as evidence of the complex magnetic order in Ru-1222. We propose a specific multilayer model to explain the data, and note that superconductivity in the ruthenocuprate is compatible with both the presence and absence of the magnetic dynamics.

DOI: 10.1103/PhysRevB.65.144420 PACS number(s): 74.72.Jt, 74.25.Ha, 75.60.Lr, 75.70.Cn

I. INTRODUCTION

Coexistence of superconductivity and long-range magnetic order, and the types of magnetic order compatible with superconductivity, are problems of widespread interest.[1] Such systems include the ruthenocuprates, which exhibit superconductivity in the CuO_2 planes[2] with some type(s) of long-range magnetic order that involves at least the RuO_2 planes.[3,4] One of the main issues for the ruthenocuprates is the nature of long-range magnetic order coexisting with superconductivity. The issue is complicated because, as previous work (muon spin rotation,[4] magnetic resonance,[5] and neutron diffraction[6]) has shown, there is evidence—even in the simple Ru-1212 material—for both ferromagnetic[4,5] and antiferromagnetic[6] ordering. Both magnetization[7] and NMR (Ref. 2) studies of Ru-1212 materials confirm the presence of a ferromagnetic component of the low temperature magnetic order. Theoretical calculations[8] of the electronic structure predict antiferromagnetic order for Ru-1212.

There is an implicit assumption that all ruthenocuprates will possess the same long-range magnetic order. As we show below, this is not the case for the data we measured, comparing Ru-1212 and Ru-1222, nor is it the case for the existing literature. To our best knowledge, neutron-diffraction measurements have not been reported for Ru-1222. Magnetization, low-frequency susceptibility, and Mössbauer/nuclear quadrupole resonance reports[3,9] indicate a pronounced—perhaps even a dominant—role of ferromagnetism in the spontaneous magnetic order of Ru-1222. The main result of our report is that Ru-1222 samples exhibit unexpected dynamical magnetic features in very low magnetic fields. We have measured the ac susceptibility while varying the dc magnetic field either continuously or in steps. We found a pronounced susceptibility ''switching,'' logarithmic time relaxation, and hysteretic, inverted-in-sense, susceptibility butterfly loops. While these properties have been individually reported earlier in other, nonsuperconducting magnetic systems, the Ru-1222 system exhibits all of these properties. The inverted butterfly hysteresis represents, to our knowledge, the first observation of this phenomenon in a bulk magnetic system. The contrast between Ru-1222 and Ru-1212 (or $SrRuO_3$) samples is marked: neither Ru-1212 nor $SrRuO_3$ exhibit any of these dynamical magnetic properties. Following the data, we present a model in which we argue that the magnetic ordering of Ru-1222 involves both ferromagnetic and antiferromagnetic coupling, and that Ru-1222 is a rare example of an intrinsic, naturally grown magnetic multilayer system with the layers coupled with antiferromagnetic interactions, similar to that inferred of the $(La,Sr)_3Mn_2O_7$ colossal magnetoresistance manganite.[10]

II. EXPERIMENT

Polycrystalline samples of Ru-1222, Ru-1212, and $SrRuO_3$ were fabricated as published elsewhere.[3,11] Two Eu/Ce stoichiometries of Ru-1222 were synthesized: ''superconducting'' (Ce content $x=0.5$) and ''insulating'' (Ce content $x=1.0$). $SrRuO_3$ served as a three-dimensional, ferromagnetic reference material. In all three materials, magnetic order stems from the RuO_6 octahedra. We used x-ray diffraction (data not shown) to establish that all samples were crystallographically single phase. We measured the sample microstructure using scanning electron microscopy, with results shown in Fig. 2 below. ac susceptibility data were taken using a CryoBIND system[12] calibrated for absolute susceptibility results. The ac susceptibility measurements used a frequency of 230 Hz, an ac magnetic field of 0.15 Oe, and a dc magnetic field between 0 and 100 Oe. dc susceptibility measurements of some samples were obtained using a Lake Shore vibrating-sample magnetometer (VSM).

III. RESULTS

Figure 1 illustrates the Ru-1222 unit cell. Notice the large separation along the c axis between RuO_2 planes; we return to this point below. Figure 2 illustrates the microstructure. Ru-1222 ($x=1.0$) samples exhibit a dense structure with almost no isolated grains and very small intergranular regions;

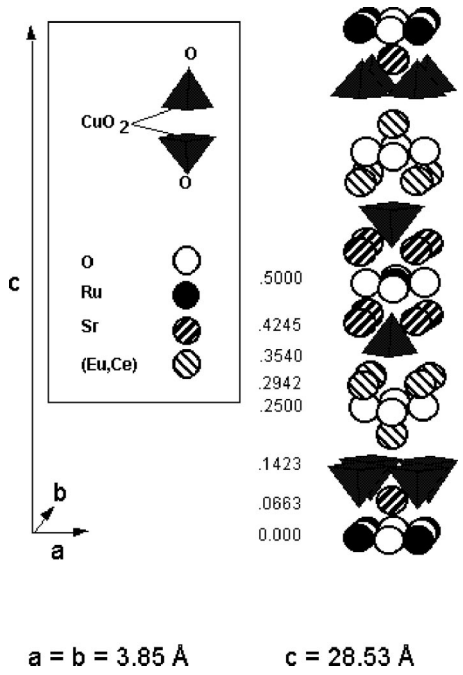

FIG. 1. Unit cell of Ru-1222 ruthenocuprate.

grain boundaries were difficult to identify. Ru-1222 ($x=0.5$) and Ru-1212 samples, by contrast, exhibit well-defined grains (size typically $1-2$ μm) and pronounced grain boundaries. As we note further below, there are marked, qualitative differences between the Ru-1212 samples and Ru-1222 samples of either stoichiometry. Figure 2 is thus important because it rules out grain structure as the source of these qualitative differences.

Figure 3 shows the ac susceptibility data of Ru-1212, Ru-1222 ($x=0.5$), and Ru-1222 ($x=1.0$). Ru-1212 exhibits a single maximum at $T_N=133$ K. By contrast, both Ru-1222 samples exhibit peaks at lower temperature $T_M[=85$ K($x=0.5$) and 117 K ($x=1.0$)] and a broad feature between 120 and 140 K, followed by non-Curie-Weiss behavior extending up to 180 K. Possible interpretations of the latter behavior as well as Ce-dependent features of magnetic order are reported elsewhere.[13]

In this work we primarily focus on the magnetically ordered ($T<T_M$) phase of both ruthenocuprates and report hysteretic and highly nonlinear magnetic dynamics characterizing Ru-1222, but not Ru-1212, samples. Figures 4–10 illustrate different aspects of the ac susceptibility response of Ru-1222, pointing out the differences in the equivalent response of Ru-1212 under similar experimental conditions. Although we show only the results for $x=0.5$ or $x=1.0$ compositions of the Ru-1222 ruthenocuprate in a particular figure, both stoichiometries exhibit the same qualitative behavior in all respects. We first report on ac susceptibility temperature dependence in small (<100 Oe) applied dc magnetic fields. Figures. 4 and 5 illustrate a sequence of temperature dependencies of zero-field cooled (ZFC) ac susceptibility measurements in several dc magnetic fields at temperatures near the peak value for Ru-1222 ($x=0.5$ and $x=1.0$) samples. These figures show that there is a range of dc magnetic field values, and temperatures, for which the ac

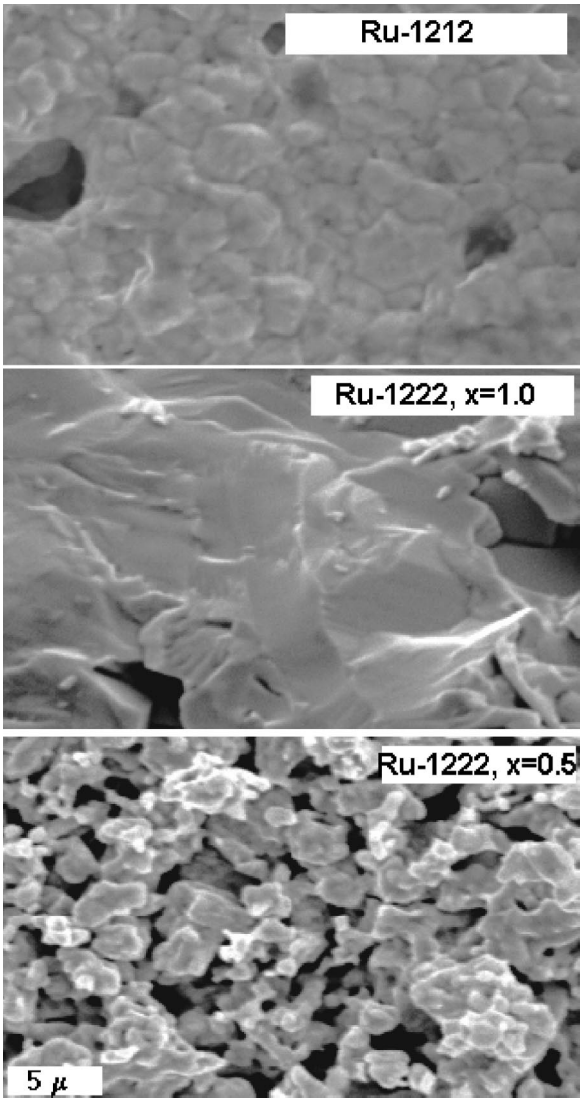

FIG. 2. Scanning electron microscopy images of Ru-1212 (top panel); Ru-1222, $x=1.0$ (middle panel); and Ru-1222, $x=0.5$ (bottom panel).

susceptibility of Ru-1222 samples increases as the dc magnetic field increases. By contrast, Ru-1212 and $SrRuO_3$ samples exhibit ''normal'' behavior: at all temperatures, the ac susceptibility monotonically decreases for increasing dc magnetic fields. Qualitatively, ''normal'' behavior is easy to interpret: ac susceptibility measures how free the magnetic moments are to perform forced oscillations imposed by the ac magnetic field. Therefore, any superimposed dc magnetic field introduces a further restriction on the oscillations, and the ac susceptibility decreases. Figure 5 illustrates ac susceptibility for Ru-1222 ($x=1.0$) samples. Note the common qualitative trend shown in Fig. 4: below T_M the ac susceptibility versus dc magnetic field exhibits nonmonotonic behavior with increasing dc magnetic field, while for temperatures above T_M the ac susceptibility decreases monotonically with increasing dc magnetic field. The unexpected increase in ac susceptibility from zero dc field to the ''turning field'' (the dc field at which the ac susceptibility is at a maximum) reaches as much as 15% for Ru-1222 ($x=1.0$). It is much less

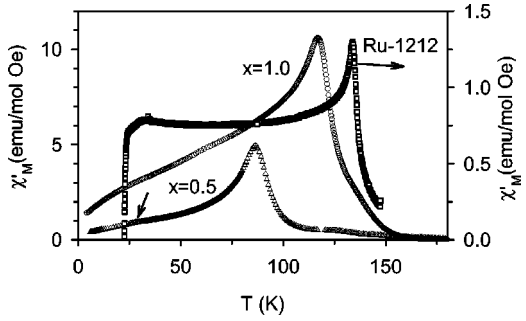

FIG. 3. ac susceptibility measurements of Ru-1222 ($x=0.5$ and $x=1.0$) and Ru-1212 samples. Note different scales for the two sample types. Vertical arrow indicates the kink attributed to superconductivity in the Ru-1222, $x=0.5$ sample.

($\approx$0.5%) for Ru-1222 ($x=0.5$), and the magnitude of the turning field is lower for Ru-1222 ($x=0.5$) than for Ru-1222 ($x=1.0$). For some samples we also noted small, quasiperiodic jumps in the temperature dependence of the ac susceptibility below T_M, similar to the jumps recently reported for certain manganite samples.[14] Because the occurrence of these oscillations/jumps was not reproducible in repeated measurements, we did not perform any systematic studies of this effect on our samples.

A. Time dependence of ac susceptibility

We measured the time response of the ac susceptibility to different dc magnetic fields at several fixed temperatures. We would zero-field cool the sample to a fixed temperature, apply a dc field, and take the measurement of time dependence, then—in zero dc magnetic field–raise the temperature to above 180 K and lower the temperature (to the same or another fixed temperature) before repeating the measurement with different dc field. Figure 6 illustrates a sequence of ZFC measurements in several increasing dc fields. The way in which the dc magnetic field was abruptly turned on and off has been also shown. Figure 6 shows that the ac susceptibility sharply increases (''switches'') when the dc magnetic field is turned on. After the ac susceptibility switch, there is a gradual decrease. In Fig. 6 the time window of only 500 s is shown; we note however that ac susceptibility does not usually return to the initial ZFC value on the time scale of at least one day (the longest period we measured at one dc field and temperature).

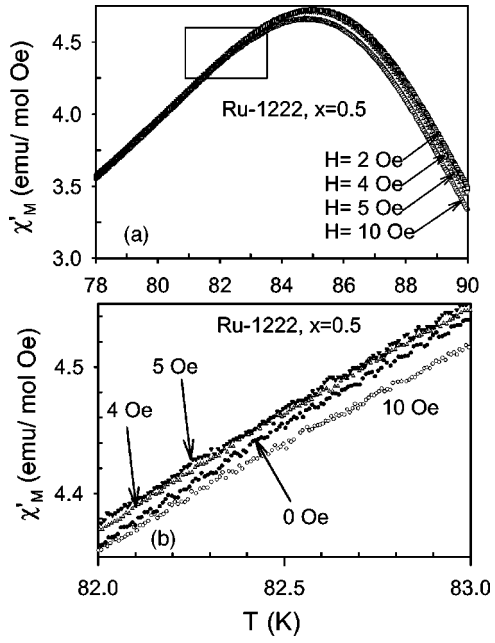

FIG. 4. Temperature dependence of ZFC ac susceptibility of Ru-1222, $x=0.5$ sample in a sequence of small applied magnetic fields. (a) would suggest collapsing of all of the curves below the ordering maximum inside the 10 Oe magnetic-field range. A closer inspection of the rectangular area, shown in (b) on an expanded scale, indicates that below the ordering maxima there is actually a nonmonotonic change of ac susceptibility as the applied magnetic field increases.

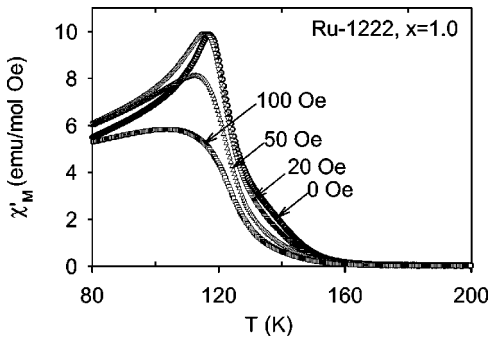

FIG. 5. Temperature dependence of ZFC ac susceptibility of Ru-1222, $x=1.0$ sample versus applied dc magnetic field. Below the ordering maxima, the susceptibility exhibits nonmonotonic behavior versus applied magnetic field.

The ac susceptibility exhibits a strong time relaxation. Such relaxation–often called disaccommodation[15,16]—has been reported previously for other magnetic systems.[15] The data in Fig. 6 are, however, surprising in certain respects: the ac susceptibility *increases* above the ZFC value when a dc magnetic field is applied. One observes the latter increase as long as the applied dc field amplitude is small enough (smaller than, approximately, 65 Oe, under the conditions defined in Fig. 6). Also, if the applied field is big enough, switching it off triggers a sizable susceptibility jump to the ac susceptibility level bigger than any previous one. In particular, the data indicate the following:

(1) A steplike change of the dc magnetic field causes (i) the ac susceptibility to switch to a new value, and (ii) the ZFC equilibrium state to change to a metastable magnetic state. The magnitude of the ac susceptibility change ($\Delta\chi$) (Fig. 6) is positive when H_{dc} is turned on, and can be either positive or negative when H_{dc} is turned off. The metastable magnetic state exhibits logarithmic relaxation [Fig. 7(a)], a phenomenon variously ascribed to disaccommodation[15,16] or magnetic aftereffect.[17]. It is particularly noteworthy, as Fig. 7(b) illustrates, that Ru-1212 samples do not exhibit any indication of ac susceptibility relaxation

(2) The ac susceptibility relaxation is logarithmic in time for both H_{dc} on and H_{dc} off, and follows the functional form $\chi(t)=\chi_0[1-\alpha\ln(t-t_0)]$. The parameters χ_0 and the relax-

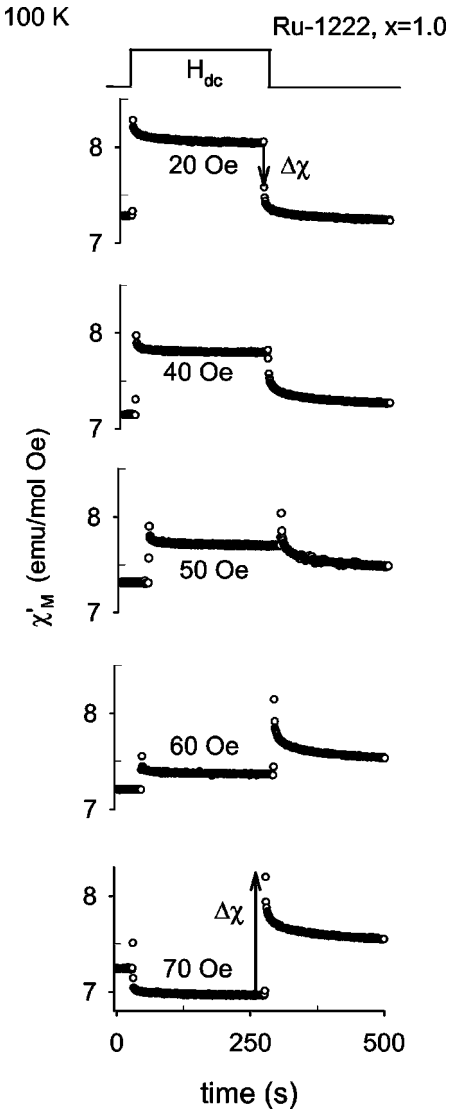

FIG. 6. Sequence of ac susceptibility versus time measurements for Ru-1222, $x=1.0$ at 100 K, in several dc magnetic fields (H_{dc}). $H_{dc}=0$ Oe initially, then acquires one of the designated values, and finally swtiches back to zero, as shown schematically at the top of figure. Overshoot ($\Delta\chi$), defined as a change in susceptibility immediately after H_{dc} is switched off, can be both negative and positive, depending on the H_{dc} value [inset to Fig. 7(a)].

ation rate α depend on temperature, H_{dc}, and the magnetic history (whether H_{dc} was turned on or off)

(3) For $|H_{dc}|$ above a threshold value H_t ($\approx$40 Oe for data of Fig. 6), when H_{dc} is turned off there is a pronounced ''overshoot'' phenomenon with a sizeable positive ($\Delta\chi$) [see inset to Fig. 7(a)]

(4) Surprisingly, applying a rectangular field pulse of magnitude $H>H_t$ results in a magnetic state with an *increased* ac susceptibility (Fig. 6). The logarithmic relaxation over several decades of time indicates that the excited ac susceptibility persists on a long term basis. We point out that nonmonotonic behavior of ZFC ac susceptibility in increasing dc fields (Fig. 6) is fully compatible with similar observations characterizing the temperature dependencies of ac susceptibility (Figs. 4 and 5) of the same samples below T_M.

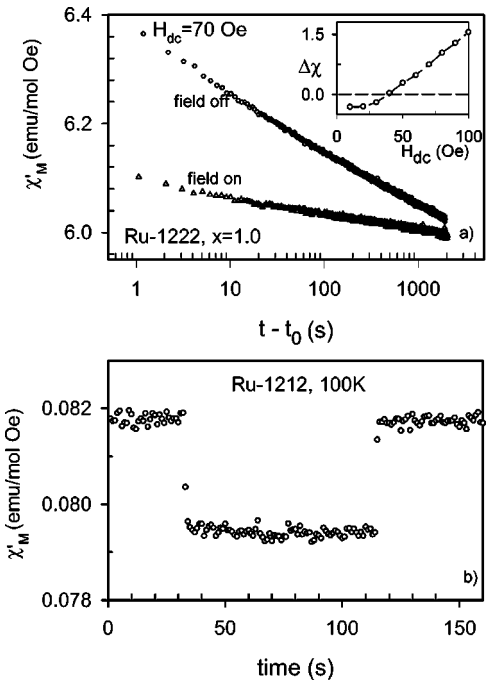

FIG. 7. (a) ac susceptibility versus logarithm of time for Ru-1222, $x=1.0$, with $H_{dc}=70$ Oe at 80 K. (t_0) is time at which H_{dc} is either switched on or off. Data for both *field on* and *field off* conditions are included. Inset: Overshoot $\Delta\chi$ (in units of emu/mole Oe) at 80 K versus H_{dc}. Note change from negative (no overshoot) to positive (overshoot) at $H_{dc}=H_t$. (b) ac susceptibility versus time for Ru-1212 at 100 K in the applied rectangular pulse of magnetic field, as specified in Fig. 6. No time relaxations can be detected in the Ru-1212 sample.

B. ac susceptibility in sweeping magnetic field: Observation of inverted hysteresis

We also swept the dc magnetic field in an almost continuous fashion, with increments typically of 1 Oe. The most striking behavior, as shown in Fig. 8, is an inverted hysteresis phenomenon for Ru-1222 that is also entirely absent for Ru-1212 or $SrRuO_3$. To measure the classic magnetization hysteresis, one ramps the applied magnetic field (H) from positive to negative and back, and continuously measures the magnetization $M(H)$. In a similar, ''butterfly'' hysteresis technique,[18] the ac susceptibility $\chi_{ac}(H)$ is measured rather than the magnetization. Generally, these two hysteresis loops yield similar information.[19] For instance, the characteristic maxima in butterfly hysteresis (Figs. 8 and 9) define the coercive field.[18] Figure 8(a) shows typical butterfly hysteresis data taken for Ru-1222 and Ru-1212 samples. The data establish that the two types of ruthenocuprates exhibit qualitatively different responses. There are also pronounced differences between the Ru-1222 data and the results for $SrRuO_3$ [Fig. 9(a)]. The most striking difference is the inverted sense of loop circulation for Ru-1222: the ac susceptibility signal is consistently larger for the field-decreasing branch compared to the field-increasing branch. To our knowledge, this is the first observation of inverted butterfly loops in a bulk magnetic system. The numerical integration of the butterfly hysteresis is shown for Ru-1222 [Fig. 8(b)] and $SrRuO_3$ [Fig.

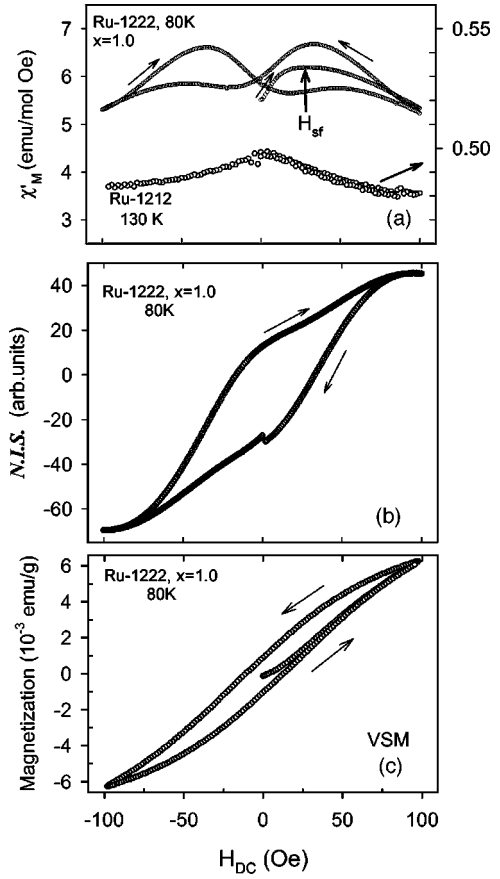

FIG. 8. (a) Left axis: ''Butterfly'' hysteresis for Ru-1222, $x=1.0$ at 80 K. Right axis: Analogous data for Ru-1212, just below magnetic ordering temperature. Unlike Ru-1222, note for Ru-1212 a monotonic decrease in ac susceptibility with increasing magnitude of the dc magnetic field, and no hysteresis. (b) Numerical integral NIS $[\equiv\int_0^H \chi(h)dh]$ of butterfly susceptibility shown in (a) versus H_{dc} for Ru-1222. The units are arbitrary. Note the inverse hysteresis loop. (c) dc (vibrating-sample) magnetization hysteresis for the same Ru-1222 sample as in (a). A normal (counterclockwise) circulation is observed.

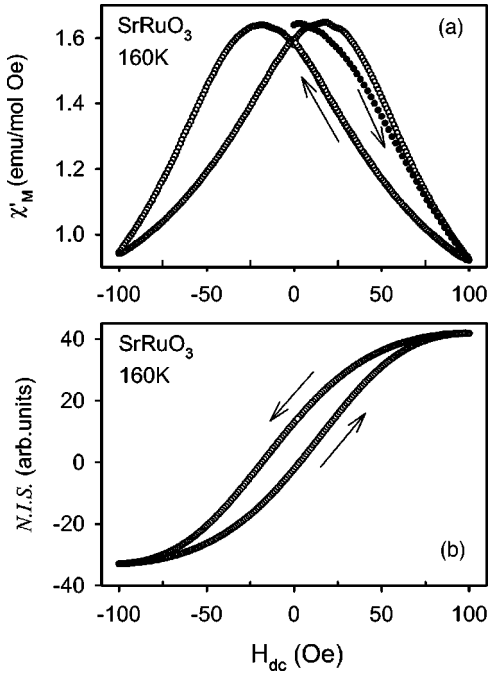

FIG. 9. (a) Butterfly hysteresis for the reference ferromagnet $SrRuO_3$ at 160 K (i.e., just below $T_c=165$ K, its ordering temperature). Filled circles designate the virgin hysteresis branch, characterized by no maximum or other features. Note that the responses for increasing and decreasing H_{dc} are opposite to that of Ru-1222. (b) NIS for $SrRuO_3$ at 160 K. Note that this hysteresis corresponds, by all means, to the standard ferromagnetic one.

9(b)]. While the results for $SrRuO_3$ exhibit the counterclockwise pattern of the usual magnetization hysteresis, the integrated butterfly of the Ru-1222 sample exhibits an inverted (clockwise) hysteresis loop. It is noteworthy that the vibrating-sample magnetometer measurements on the same Ru-1222 [Fig. 8(c)] show the dc magnetization hysteresis loop with a ''normal'' (counterclockwise) sense of circulation. Therefore, the inverted hysteresis phenomenon represents a unique, dynamical feature of the Ru-1222 system, arising from the field-induced and ac magnetic-field-assisted metastable magnetic states observed in Fig. 6. Other noteworthy features of the Ru-122 butterfly hysteresis include (i) the presence of a maximum even in the ZFC (virgin) curve, (ii) pronounced dependence on the observing time used to obtain the data, and (iii) the presence of two—rather than the expected one—maxima per field-increasing or field-decreasing branch. As Fig. 8(a) shows, the virgin branch exhibits a maximum at a characteristic dc magnetic field (H_{sf}). In simple ferromagnets, the virgin curve typically does not exhibit a maximum[20] because the remanence, and thus coercive field,[19] builds up only after the first field swing, as shown for $SrRuO_3$ [Fig. 9(a)]. The quantitative size of the butterfly hysteresis loop depends on the observation time, which is another indication that the metastable magnetic states are involved. Qualitatively, though, over the range of sweep times we studied (one minute to one day), the inverted butterfly loops exhibit the same features. Also noteworthy is that the field H_{sf} is close to the minimum field needed to apply in order to obtain closed butterfly loops: if the range of sweeping field was narrower than $(-H_{sf},+H_{sf})$ no closed loops would be observed what so ever. Instead, the ac susceptibility signal would merely systematically diminish from cycle to cycle. Figure 10(a) illustrates how H_{sf} and α_{off}, the logarithmic relaxation rate, change with temperature. The two parameters—logarithmic relaxation and inverted hysteretic behavior—exhibit virtually identical temperature dependence, indicating that the two phenomena have a common origin in Ru-1222. Another indication that the two phenomena are interrelated is shown in Fig. 10(b). α_{off} changes rapidly in small dc magnetic fields, but saturates at $H_{dc}\geqslant H_{sf}$. Another commonality is the change of $\Delta\chi$ with H_{dc} [Fig. 7(a), inset]. $\Delta\chi$ becomes positive and monotonically increaes above a threshold field previously designated as H_t. Experimentally, the two characteristic fields of the time relaxation (H_t) and butterfly hysteresis (H_{sf}) measurements acquire very close values and similar temperature dependencies, indicating that they are actually equal. The common characteristic field is interpreted below as a field associated to the spin-flop phenomenon.

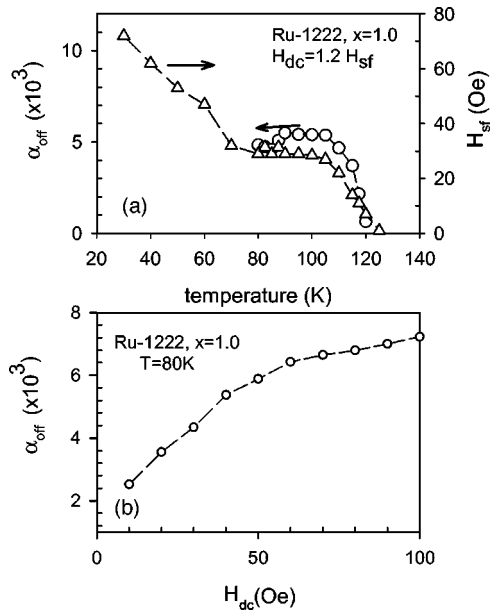

FIG. 10. (a) Left axis: α_{off}, the relaxation rate constant defined in text, when H_{dc} is switched off, versus temperature. Right axis: The field attributed to spin flop, H_{sf} [Fig. 8(a)], versus temperature. Note that both quantities are zero at temperatures above the susceptibility peak. (b) α_{off}, at 80 K, versus H_{dc}.

IV. DISCUSSION

The first step to interpreting these results is to determine whether the results are intrinsic or extrinsic. The samples are polycrystalline, so extrinsic sources can include magnetic dynamics of single domain grains with intergranular magnetic interactions. A similar question has arisen[21,22] in studies of polycrystalline $(La,Sr)_3Mn_2O_7$. For our samples, the microstructure (Fig. 2) indicates that the phenomena are intrinsic. The largest effects were measured on Ru-1222 ($x=1.0$) samples having barely detectable grain boundaries with large and densely packed crystalline grains. The effects are present in Ru-1222 ($x=0.5$) but absent in Ru-1212, although these samples have very similar microstructures with grain sizes of $1-2$ μm and pronounced grain boundaries. We conclude that the phenomena reported in Figs. 3–10 are predominantly intrinsic, due to magnetic interactions within the unit cell. The nonmonotonic ZFC ac susceptibility for different dc magnetic fields (Figs. 4 and 5) can be naturally interpreted as indicating the coexistence of antiferromagnetic (AFM) and ferromagnetic (FM) magnetic ordering in Ru-1222, with the magnetic order spontaneously occurring below T_M. As discussed further below, we argue that a small dc magnetic field partially cancels the AFM component, which increases the magnetization of the sample. This behavior leads to first an increase in ac susceptibility, with a decrease as H_{dc} increases further. A pronounced dependence of ac susceptibility on the balance between FM and AFM correlations has recently been reported[23] in $(La,Sr)_3Mn_2O_7$. Reference 23 reports the onset and growth of AFM correlations, accompanied by a remarkable drop in the ac susceptibility, which is consistent with our interpretation. One noteworthy difference between our report and Ref. 23 is that in Ru-1222, the AFM contribution is tuned by the dc magnetic field, while in Ref. 23 the AFM correlations are controlled by varying the stoichiometry. In contrast to Ru-1222, Ru-1212 exhibits a monotonic decrease of the ac susceptibility with increasing dc magnetic field. In Ru-1212, Ref. 6 argues from neutron-scattering data that there is a *G*-type AFM spontaneous magnetic order. We argue that applying a small (0–100 Oe) dc magnetic field to Ru-1212 is not large enough to induce any FM order, while such small fields are sufficient in Ru-1222. The butterfly hysteresis data provide information about the nature of the AFM component of magnetic order. For Ru-1222, the hysteresis loop from ac susceptibility data is inverted. A theoretical model for such inverted hysteresis loops[24] indicates that inverted hysteresis loops can arise in exchange-coupled layered magnetic ''sandwiches'' provided that the intralayer coupling is significantly larger than the interlayer coupling. The demagnetizing boundary effects, present in any real finite-size sample, was explicitly taken into account and shown to be crucial for the model predictions. Reference 24 also calculated the conditions needed to assure that such inverted hysteresis loops do not violate the second law of thermodynamics. Previous experimental reports of inverted hysteresis loops[25,26] have been limited to magnetic multilayers and nanoscale magnetic films. Reference 25 argues that in their samples adjacent layers have magnetic moments with AFM coupling between adjacent layers. Reference 25 also demonstrated that the inverted hysteresis loop behavior disappears in their samples if the AFM interlayer coupling is changed to a FM interlayer coupling. The present report, to our knowledge, is the first to show inverted hysteresis loops for bulk magnetic systems. We argue that the presence of such inverted hysteresis loops in Ru-1222 arises from RuO_2 layers with FM magnetic moments, combined with AFM coupling between the RuO_2 planes. A similar conclusion has recently been made for the layered manganite $(La,Sr)_3Mn_2O_7$ based on magneto-optical[10] and neutron-diffraction[27] data; in this compound the MnO_2 plays the role of the FM layers.

Observing inverted hysteresis loop behavior provides support for a magnetic multilayer scenario in Ru-1222. Arguing for AFM interlayer coupling, however, requires more specific experimental support. The most direct support would be evidence of a spin-flop transition through which the net magnetization of adjacent, weakly AFM coupled, layers increases.[28] Unfortunately, to our best knowledge, there are no single-crystal samples of Ru-1222 available to obtain such direct evidence, e.g., by neutron diffraction. We argue, however, that our results support the presence of a spin-flop transition at the characteristic field H_{sf} in favorably oriented grains of our polycrystalline Ru-1222 samples. It is important to note that the butterfly hysteresis loops we measured would close only for applied fields larger than H_{sf}, which is consistent with a spin-flop transition and the onset of irreversible behavior. We attribute the maxima in the initial ac susceptibility data [Fig. 8(a)] to a spin-flop transition. This assignment is quite similar to a recent report on AFM ordered chain-ladder compounds.[29] In Ref. 29, the position of the susceptibility peak defines the spin-flop field. This field is substantially higher in Ref. 29 than in this report due to the different

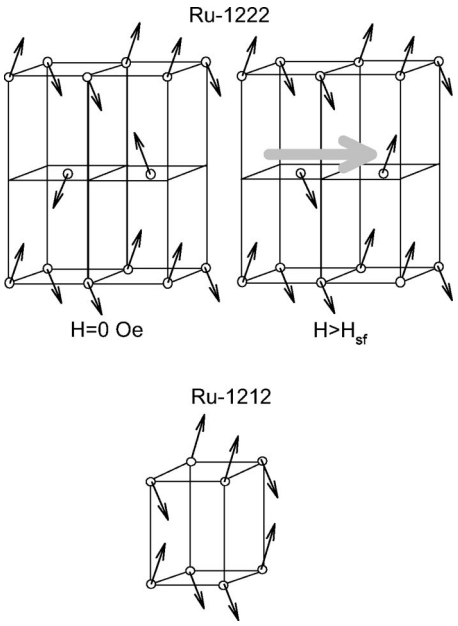

FIG. 11. Model for magnetic structure of Ru-1222. The region, two unit cells wide, is shown schematically. Circles designate the Ru ions and arrows the associated magnetic moments. A widely accepted model (Ref. 30) for the magnetic structure of Ru-1212 is also shown for comparison. The global order is *G*-type antiferromagnetic in both systems. In Ru-1222, small ferromagnetic components—a projection of the moments to the RuO_2 planes—are antiparallel in $H=0$. The in-plane components become mutually parallel—ferromagnetic—by application of small spin-flop field H_{sf}. Thick grey arrow designates the field direction.

nature of AFM interactions in the two systems. However, our experimental values of a spin flop field below 100 Oe are compatible with the field values measured in magnetic trilayer and multilayer systems, which are several orders of magnitude smaller than bulk AFM systems.[28]

A. Model for magnetic coupling in Ru-1222

While our report does not include any determination of the magnetic structural order, the results are compatible with a simple model, shown schematically in Fig. 11. We start with the generally accepted model for the magnetic structure of the more thoroughly investigated, and simpler, Ru-1212. It is well established[6,30] that the dominant magnetic order is a *G*-type antiferromagnetic structure in which the Ru moments are aligned antiparallel in all crystallographic directions. The details of the magnetic order and the stability of a particular ground state[8] can be interpreted only by explicitly including rotations and tilting of the RuO_6 octahedra and considering the orientation of the magnetic moments. A weak ferromagnetism originates from canting the Ru moments.[3] The canting arises from the Dzyaloshinsky-Moriya[31] antisymmetric superexchange interaction which, by symmetry, follows from the fact that the RuO_6 octahedra tilt away from the crystallographic *c* direction; there is still *a* controversy as to whether the tilting around the axis perpendicular to the c-axis is actually observed.[9,30,32] In Ru-1212 samples containing magnetic (Gd) ions, the dipolar field of the in-plane ferromagnetic components induces an additional ferromagnetic component.[7,30] Very recently, results of a structural investigation of the Ru-1222 compound ($x=1.0$) indicates that there are no important differences in rotation or tilting angles between the Ru-1212 and Ru-1222 ($x=1.0$) compounds,[9] in spite of Ru-1212 exhibiting dominant antiferromagnetic and Ru-1222 dominant ferromagnetic spontaneous magnetic order. We suggest that the magnetic ordering in both compounds is a variation of the *G*-type antiferromagnetism, while variation in dc magnetic properties, particularly in low fields, arises from small differences in the Ru-Ru interaction within their respective unit cells. The unit cells are different: in Ru-1222 there is a structural phase shift of half of the RuO_2 planes that leads to an approximate doubling of the unit cell. The phase shift arises from the presence of the fluorite-structure block $Eu_{2-x}Ce_xO_2$ replacing the rare-earth ion in Ru-1212. Thus, in Ru-1222, nearest-neighbor (Ru) ions are not vertically aligned, while they are in Ru-1212. This difference in structure naturally leads, in Ru-1222, to having the relative alignment of the in-plane components in adjacent RuO_2 planes antiparallel, which is energetically favored by a bare dipole-dipole interaction. Figure 11 shows the magnetization tilting scheme we propose for Ru-1222. Our experimental results fit quite naturally with such a picture: since the dipole interaction is very weak—the energy needed to reverse the in-plane Ru moment component is small—a small applied magnetic field can easily transform the spontaneous AF order, via a spin-flop mechanism, into a ferromagnetic orientation. This is exactly what our measurements indicate. Our model is, apart from the unusual dipole-dipole interaction, the same as the models used to explain weakly AF coupled magnetic multilayers.[28,33] We note that our model does not take into account the role of the (Ce), which is expected to have a nonzero magnetic moment. Our model is, however, of use in understanding the qualitative features of the Ru-1222 experimental data.

The most unusual feature of our model is the pronounced role of the dipole-dipole interaction; various magnetic exchange interactions (e.g., superexchange, double exchange) are more commonly employed to explain magnetic coupling. We argue that a dipole-dipole interaction makes sense because the nearest RuO_2 layers are far apart, with insulating and nonmagnetic layers in between. Experimentally, the logarithmic time dependence of the magnetic relaxation [Fig. 7(a)] argues for the long-range dipole-dipole interaction; it is well known[34] that such a long-range interaction can account for a logarithmic relaxation behavior without further assumptions. We also considered the possibility that the logarithmic relaxation behavior might be due to domain-wall stabilization (disaccommodation) involving a broad range of activation energies, as has been recently applied to data in a perovskite manganite.[14,16] However, one of us (I.F.) and colleagues have performed temperature-dependent x-ray diffraction studies of Ru-1222.[35] The measurements indicate no structural change with temperature—such changes are necessary for disaccommodation. Thus both the weak AF coupling and the logarithmic susceptibility relaxation support our model.

V. CONCLUSION

In summary, we have presented data indicating that Ru-1222 exhibits a variety of magnetic behaviors, including magnetic logarithmic relaxation, inverted hysteresis loops, and metastable magnetic states. None of these behaviors are observed in Ru-1212. Our results are interpreted within a model for the magnetic structure for Ru-1222 that, assuming a *G*-type AF global magnetic order known to describe Ru-1212, attributes the interlayer magnetic coupling to a dipole-dipole interaction. We interpret the hysteretic behavior as similar to that reported for magnetic multilayers, trilayers, and some manganites, due to spin-flop transitions converting the spontaneous ($H=0$) AF order between components into a ferromagnetic order.

Note added. After completion of this work and after the original version of the manuscript was submitted in short form,[36] we became aware of two reports that are related to our report, including the work by Ohkoshi *et al.*[37] on spin-flip transitions in bulk materials, and by Xue *et al.*[38] on $RuSr_2(Gd,Ce)_2Cu_2O_{10-y}$ using magnetization.

ACKNOWLEDGMENTS

We benefited from conversations with Robert Joynt. We also thank K. Zadro for the VSM measurements. Financial support was partially provided by the U.S.- Israel Binational Science Foundation, the U.S. D.O.E., the SCOPES program of the Swiss National Science Foundation, Fonds National Suisse de la Recherche Scientifique, and EPFL.

*Electronic address: prester@ifs.hr
†Electronic address: onellion@landau.physics.wisc.edu

[1] Superconductivity in Ternary Compounds, edited by M.B. Maple and O. Fischer (Springer-Verlag, Berlin, 1982).
[2] Y. Tokunaga, H. Kotegawa, K. Ishida, Y. Kitaoka, H. Takigiwa, and J. Akimitsu, Phys. Rev. Lett. **86**, 5767 (2001).
[3] I. Felner, U. Asaf, Y. Levi, and O. Millo, Phys. Rev. B **55**, R3374 (1997).
[4] C. Bernhard, J.L. Tallon, Ch. Niedermayer, Th. Blasius, A. Golnik, E. Brücher, R.K. Kremer, D.R. Noakes, C.E. Stronach, and E.J. Ansaldo, Phys. Rev. B **59**, 14 099 (1999).
[5] A. Fainstein, E. Winkler, A. Butera, and J. Tallon, Phys. Rev. B **60**, R12 597 (1999).
[6] J.W. Lynn, B. Keimer, C. Ulrich, C. Bernhard, and J.L. Tallon, Phys. Rev. B **61**, R14 964 (2000).
[7] G.V.M. Williams and S. Krämer, Phys. Rev. B **62**, 4132 (2000).
[8] K. Nakamura, K.T. Park, A.J. Freeman, and J. Jorgensen, Phys. Rev. B **63**, 024507 (2001).
[9] G.V. Williams *et al.*, cond-mat/0108521 (unpublished).
[10] U. Welp, A. Berger, D.J. Miller, V.K. Vlasko-Vlasov, K.E. Gray, and J.F. Mitchell, Phys. Rev. Lett. **20**, 4180 (1999).
[11] H. Berger *et al.* (unpublished).
[12] See http://www.cryobind.com
[13] Y. Hirai, I. Zivkovic, B.H. Frazer, A. Reginelli, L. Perfetti, D. Ariosa, G. Margaritondo, M. Prester, D. Drobac, D.T. Yiang, Y. Hu, T.K. Sham, I. Felner, M. Pederson, and M. Onellion, Phys. Rev. B **65**, 054417 (2002).
[14] M. Muroi, R. Street, J.W. Cochrane, and G.J. Russell, Phys. Rev. B **64**, 024423 (2001).
[15] H. Kronmüller, Philos. Mag. B **48**, 127 (1983).
[16] M. Muroi, R. Street, J.W. Cochrane, and G.J. Russell, Phys. Rev. B **62**, R9268 (2000).
[17] R. Street and S.D. Brown, J. Appl. Phys. **76**, 6386 (1994).
[18] F.H. Salas and D. Weller, J. Magn. Magn. Mater. **128**, 209 (1993), and references therein.
[19] The equivalency of butterfly and magnetization hysteresis is a simple consequence of the relationship $M(H)=\int_0^H \chi(h)dh$, valid—up to an integration constant—in simple isotropic ferromagnets. However, in complex magnetic systems, replacing χ (a tensor) by a scalar is not approved and the relationship does not hold.
[20] In principle, the observed maximum could be ascribed to a crossover between reversible and irreversible dynamics of ferromagnetic domains. However, the idea of reversibility, at least in its elementary form, is incompatible with logarithmic relaxations characterizing the whole 0—100 Oe range. Therefore, it seems that the latter interpretation cannot be applied in its original transparent form.
[21] A. Gupta, G.Q. Gong, G. Xiao, P.R. Duncombe, P. Leceoeur, P. Trouilloud, Y.Y. Wang, V.P. Dravid, and J.Z. Sun, Phys. Rev. B **54**, R15 629 (1996).
[22] H.Y. Hwang, S-W. Cheong, N.P. Ong, and B. Batlogg, Phys. Rev. Lett. **77**, 2041 (1996).
[23] S.I. Patil, S.M. Bhagat, S.B. Ogale, Q.Q. Shu, and S.E., Lofland J. Appl. Phys. **87**, 5028 (2000).
[24] A. Aharoni, J. Appl. Phys. **76**, 6977 (1994).
[25] P. Poulopoulos, R. Krishnan, and N.K. Flevaris, J. Magn. Magn. Mater. **163**, 27 (1996), and references therein.
[26] M. Cougo dos Santos, J. Geshev, J.E. Schmidt, S.R. Teixera, and L.G. Pereira, Phys. Rev. B **61**, 1311 (2000).
[27] T.G. Perring, G. Aeppli, T. Kimura, Y. Tokura, and M.A. Adams, Phys. Rev. B **58**, R14 693 (1998).
[28] B. Dieny, J.P. Gavigan, and J.P. Rebouillat, J. Phys.: Condens. Matter **2**, l59 (1990); B. Dieny and J.P. Gavignan, *ibid.* **2**, 187 (1990).
[29] M. Isobe, Y. Uchida, and E. Takayama-Muromachi, Phys. Rev. B **59**, 8703 (1999).
[30] J.D. Jorgensen, O. Chmaissem, H. Shaked, S. Short, P.W. Klamut, B. Dabrowski, and J.L. Tallon, Phys. Rev. B **63**, 054440 (2001).
[31] T. Moriya, Phys. Rev. **120**, 91 (1960).
[32] A.C. McLaughlin, W. Zhou, J.P. Attfield, A.N. Fitch, and J.L. Tallon, Phys. Rev. B **60**, 7512 (2000).
[33] G.A. Prinz, Science **282**, 1660 (1998), and references therein.
[34] D.K. Lottis, R.M. White, and E.D. Dahlberg, Phys. Rev. Lett. **67**, 362 (1991).
[35] I. Felner, U. Asaf, F. Ritter, P.W. Klamut, and B. Dabrowski, Physica C **364-365**, 368 (2001).
[36] I. Žívković *et al.*, cond-mat/0107388 (unpublished).
[37] S. Ohkoshi, T. Hozumi, and K. Hashimoto, Phys. Rev. B **64**, 132404 (2001).
[38] Y.Y. Xue, D.H. Cao, B. Lorenz, and C.W. Chu, Phys. Rev. B **65**, 020511(R) (2002).